JOURNAL OF SPACECRAFT AND ROCKETS
Vol. 43, No. 6, November–December 2006

Effect of Magnetic Fields on Surface Plasma Discharges at Mach 5

Roger L. Kimmel* and James R. Hayes†
U.S. Air Force Research Laboratory, Wright–Patterson Air Force Base, Ohio 45433
and
James A. Menart‡ and Joseph Shang§
Wright State University, Dayton, Ohio 45435

DOI: 10.2514/1.14247

Longitudinal dc discharges were created between surface electrodes on a flat plate in a Mach 5 flow. Transverse magnetic fields were applied parallel to the plate surface and normal to the freestream velocity, creating Lorentz force vectors directed either into or out of the plate surface, depending on the sign of the current and magnetic field vectors. The magnitude of the magnetic field varied from 0 to 1 T, and the total current varied from 0.025 to 0.3 A. Surface pressures were measured at three locations between the electrodes. In the absence of any applied magnetic field, the discharge increases surface pressure through boundary-layer heating and subsequent viscous interaction. An applied magnetic field clearly affects the surface pressure. In general, a Lorentz force vector directed into the plate surface inhibited surface pressure increases, and a Lorentz force vector in the opposite direction had the opposite effect. Although this is consistent with a Lorentz force, joule heating in the boundary-layer fluid is a dominating effect in the flow. It is unclear how much of the observed magnetic field effect is due to a Lorentz force, and how much is due to modification of the joule heating by the magnetic field.

Nomenclature

A	=	electrode area, 2×10^{-4} m^2
B	=	magnetic field, T
c_f	=	skin friction coefficient
E	=	electric field, V/m
e	=	electronic charge, 1.6×10^{-19} C
Ha	=	Hartmann number, $BL\sqrt{\sigma/\mu}$
I	=	interaction parameter, $(\sigma B^2 L/\rho U)(E/UB)$
I^*	=	modified interaction parameter with u^* as the velocity scale
L	=	interaction length, m
J	=	current, A
j	=	current density, A/m^2
m_e	=	electron rest mass, kg
U	=	gas velocity, m/s
u^*	=	friction velocity, $\sqrt{\tau_w/\rho_w}$
V	=	applied voltage, V
β	=	Hall parameter, $eB/(m_e \nu)$
Δx	=	streamwise distance between electrodes, 0.032 m
μ	=	gas viscosity
ν	=	electron collision frequency, s^{-1}
ρ	=	gas density
σ	=	conductivity, S/m
τ	=	skin friction

Presented as Paper 2661 at the AIAA 35th Plasmadynamics and Lasers Conference, Portland, OR, 28–30 June 2004; received 22 April 2005; revision received 27 December 2005; accepted for publication 12 January 2006.

*Senior Research Engineer. Associate Fellow AIAA.
†Senior Research Engineer.
‡Associate Professor, Department of Mechanical and Materials Engineering. Member AIAA.
§Research Professor, Department of Mechanical and Materials Engineering. Fellow AIAA.

I. Introduction

MAGNETOHYDRODYNAMIC (MHD) and non-MHD plasmas offer the potential of flow control without moving parts. The concept of applying MHD control to hypersonic flows is not new [1,2]. However, recent system concepts [3] have renewed interest in this topic, especially concepts including nonequilibrium ionization.

Control of inviscid flows, especially MHD control, is problematic due to the relatively low plasma conductivity and high velocity of hypersonic flows, leading to low interaction parameters [4]. Boundary-layer control appears more promising. Large volumes of plasma do not need to be ionized. Velocity and density are low, and applied magnetic fields are highest near the body, thus maximizing the interaction parameter. Also, because the boundary layer can amplify fluid dynamic perturbations, even small inputs can have large impact. MHD experiments on compressible [5] and incompressible [6] boundary layers have shown significant effects even at very low values of interaction parameter, based on a boundary-layer-edge velocity scale.

Boundary layers may be manipulated by the application of surface glow discharge alone, either through joule heating of the fluid or electrohydrodynamic (EHD) forces on the plasma. An advantage of this form of control over MHD control is that no magnets are required. A number of researchers have exploited EHD forces in subsonic boundary layers on flat plates using glow discharges [7], and corona discharges [8,9]. Glow discharges have been used to delay separation and enhance lift on airfoils [10–13] and to trip the boundary layer on 3-D airfoils [14]. Wilkinson [15] has explored spanwise-oscillating discharges as a means of reducing Reynolds stress and skin friction in turbulent boundary layers. At the time of this publication, EHD control has not been applied explicitly to hypersonic boundary layers. Macheret et al. [16] suggest that velocities induced by EHD effects could be appreciable at low density, but also note that joule heating effects may be hard to separate from EHD effects.

Limited results on joule heating control have been obtained in supersonic boundary layers. Analysis of surface microwave discharges [17] indicates local heating, with attendant increases in pressure and boundary-layer displacement thickness, for these flows. Leonov et al. [18–22] have considered pulsed dc discharges in subsonic, transonic, and low supersonic flows. In these experiments,

pulses of up to 10 kW and 60 ms duration are applied to electrode pairs in the wall. At lower power the boundary layers thickened, increasing wall pressure and creating a wave structure above the boundary-layer edge. Sufficiently high-power discharges separated the boundary layer and even caused choking in duct flows.

Menart et al. [23] observed that continuous surface dc discharges caused a local increase in static pressure on a flat plate at Mach 5. In this experiment, streamwise and transverse discharges were generated on a flat plate. The maximum effect was derived from the streamwise discharge, just downstream of the cathode. These results occurred even without the presence of a magnetic field, and were ascribed to joule heating of the fluid from the discharge. Heating of the boundary-layer fluid caused an increase in the boundary-layer thickness, creating a pressure increase due to viscous interaction. Magnetic fields imposed normal to the plate surface modified the pressures, but this effect was ascribed to changes in the discharge due to the magnetic field, not a Lorentz force. Later measurements by Kimmel et al. [24] confirmed this trend. This paper summarizes and expands upon the results of Kimmel et al. [24,25].

II. Description of the Experiment

A. Test Device

Tests were conducted in the Air Force Research Laboratory, Air Vehicles Directorate (AFRL/VA) plasma channel (Fig. 1). The plasma channel is a small scale, low-density channel designed for the study of plasma dynamics and magnetoaerodynamic phenomena. It consists of a two-dimensional nozzle operating at a stagnation temperature of about 270 K and a stagnation pressure range of 0.4 to 1.0 atm. The current tests were carried out at a stagnation pressure of 370 torr, with stagnation temperatures of approximately 280 K. Pitot probe measurements showed the freestream Mach number on the tunnel centerline to be $5.3 \pm 3\%$. The nozzle exit dimensions are 178 mm in height and 74 mm in width. The entire channel is fabricated from acrylic plastic and assembled with nylon screws. A test cabin houses a model support and probes. A prior publication describes the device in detail, including flow calibration [26].

The magnet used in the experiment is the GMW model 3474 electromagnet. It is a continuous-operation, water-cooled model. The magnet was run with the maximum spacing to clear the tunnel sidewalls, 160 mm, and the maximum pole-cap diameter of 250 mm. Each pole cap contained a 5-cm-diam through-hole for visual access to the test section. Under these conditions, the maximum transverse magnetic field has a magnitude of 0.9 T and is nearly uniform. The power supply may be switched to reverse the magnetic field. The magnet is rail-mounted so that it may be moved downstream to access the test section.

B. Model and Instrumentation

The model used for this study was a plate constructed of machineable ceramic with copper electrodes. Figure 2 shows a schematic. The discharge was run with the cathode either upstream or downstream. The dc discharge is provided by a Universal Voltronics reversible polarity power unit. It is rated for a maximum power output of 8 kW, a maximum voltage output of 10 kV and a maximum current output of 800 mA. All discharges were current-stabilized, i.e., the power supply modulated voltage to provide a constant current.

At a stagnation pressure of 370 torr the length Reynolds number for the plate based on freestream conditions was 9.4×10^4. The boundary layer is expected to be laminar at this Reynolds number. Pitot probe measurements made near the plate surface during stagnation pressure sweeps verified this [24].

The model contained three pressure taps on centerline, spaced 1.27 cm apart, as shown in Fig. 2. Surface pressure measurements were made with MKS Baratron pressure transducers with a 0–2 torr range. The manufacturer's stated accuracy of the transducers is $\pm 0.5\%$ of full scale. The transducers were calibrated in the laboratory and shown to be linear within 0.4%. The study reported here was phenomenological in nature. The primary objective in measuring pressures was to compare the change in pressure in the presence of a plasma to the plasma-off pressure. As such, an estimate of the accuracy of the absolute pressure reading is not crucial. What is important is the ability of the transducer to resolve small changes in pressure. After amplification, the sensitivity of the pressure measurements was approximately 2.5 V per torr. Data were digitized using a 14-bit Hewlett Packard digital voltmeter. Pressure changes due to discharges measured in this study ranged from 0.01 to 0.1 torr and thus were far above the resolution limit of the analog to digital converter and the rms noise level of the measurements, measured at approximately 0.003 torr.

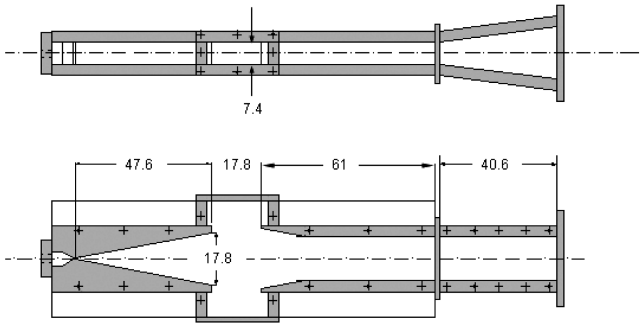

Fig. 1 Schematic of AFRL/VA Mach 5 plasma channel.

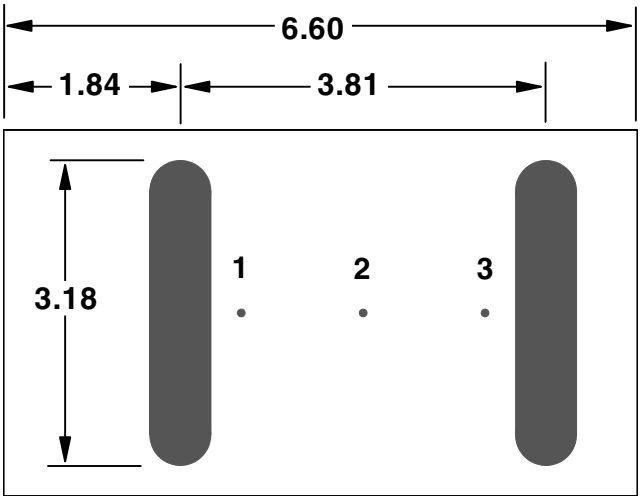

Fig. 2 Schematic of flat plate model. All dimensions cm. Electrodes are 0.64 cm wide. Pressure taps are spaced 1.27 cm, starting at $x = 2.48$ cm.

A more serious concern than the resolution of the pressure measurements is the response time of the measuring system. To avoid potential discharges through the transducers, the transducers were mounted external to the wind tunnel, and coupled to the tunnel through plastic tubing. Because of the low pressures and long lengths of tubing involved, the surface pressure response was quite lagged. The effect of this lag is described in the next section.

III. Results

A. Pressure Distribution in the Presence of a Discharge, No Applied Magnetic Field

Kimmel et al. [24] describe in detail the flat-plate surface pressure and flowfield in response to a discharge with the cathode upstream. In this case cathode-heating dominates the flowfield. This heating expands gas near the cathode and creates a compression field around it. The electrode and the surrounding plate material also heat internally and some of this heat convects into the boundary layer. In the current experiment, the surface pressure was measured for both the cathode upstream and downstream cases. Figure 3 illustrates the surface pressure as a function of time for a 50 mA discharge in the absence of a magnetic field. The plasma discharge is turned on at 20 s and turned off at 40 s. Pressure data at each tap are normalized by the

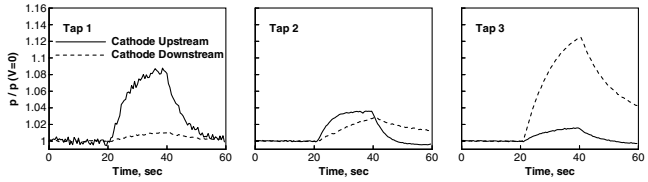

Fig. 3 Plate surface static pressure as a function of time, no magnetic field. Discharge is turned on at 20 s and turned off at 40 s.

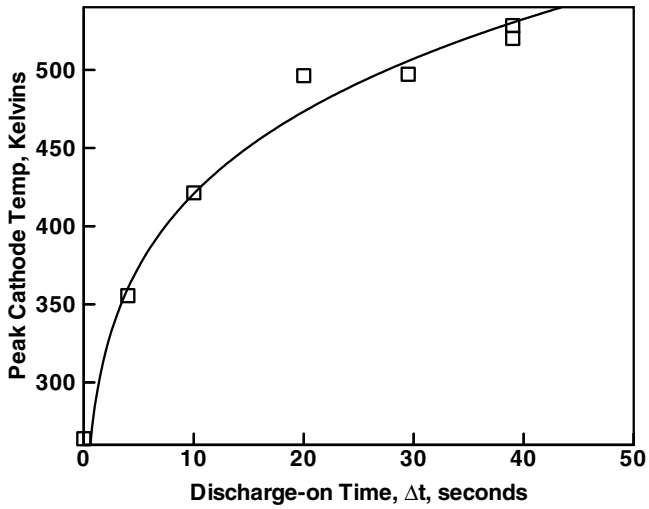

Fig. 4 Cathode peak temperature as a function of discharge-on time.

pressure in the absence of a discharge. In each case, the pressure tap nearest the cathode shows the largest pressure increase. The cathode-downstream case shows some upstream influence. This upstream influence is a combination of pressure signals propagating upstream through the boundary layer and conduction from the electrode upstream through the plate.

Temperature-sensitive paint and a thermocouple were used to estimate the time-dependent temperature of the cathode and plate. A thermocouple embedded in the cathode measured cathode temperature. A switch was used to disconnect the thermocouple from the data acquisition hardware before turning on the discharge. When the discharge was extinguished, the switch was closed to reconnect the thermocouple. A sample thermocouple signal vs time is shown in Fig. 4. This process was repeated for a variety of discharge-on times to form an approximation to the temperature vs time response of the cathode. The cathode temperature as a function of time is shown in Fig. 4. The cathode heats quickly, increasing 100 K within the first 5 s. Temperature-sensitive paint was used to visualize propagation of the temperature pulse through the ceramic plate. Before the discharge, the plate was at a nearly uniform temperature. After a 40 s discharge the plate surface temperature immediately upstream of the cathode increased as much as 50 K. Near the anode, the plate surface temperature increase was less than 10 K.

The lagged response of the surface pressures shown in Fig. 3 and the temperature response of the cathode and plate raise the question of how much of the pressure response is due to joule heating of the fluid in the discharge, and how much is due to convection from the hot cathode and plate to the fluid. An attempt was made to answer this by examining the time-response of the interaction. Before this, the time-response of the instrumentation had to be assessed. This was done by manually increasing the stagnation pressure by about 7% over 1 s. The pitot pressure response was well-described by a first-order system with a time constant of approximately 0.4 s. The surface pressure response, however, was more highly lagged, with a time constant of approximately 11 s.

The slow response of the surface pressure transducers was due to a combination of the line length, transducer internal volume, and the low static pressures. Surface pressure values reported next were

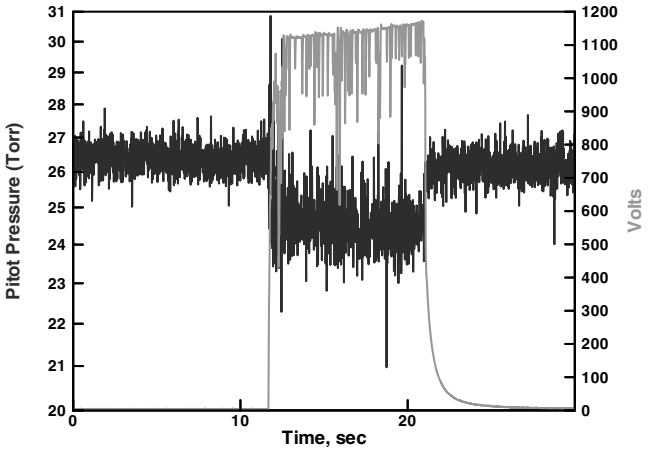

Fig. 5 Pitot pressure (black line, left scale) measured 0.5 cm above the plate surface at the downstream edge of the rear electrode, and applied electrode voltage (gray line, right scale).

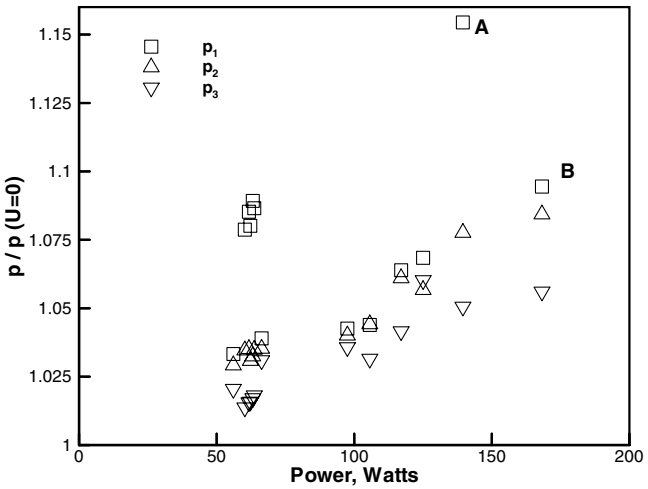

Fig. 6 Normalized surface pressure at stations 1, 2, 3 ($x = 2.48$, 3.75, and 5.02 cm, respectively) as a function of discharge input power. Pressure is normalized by discharge-off pressure.

obtained by averaging over a specified period of time. During a discharge, this was the last 10–15 s of the discharge. Discharge-on times were usually 20 s. Because the pressures in some cases had not fully equilibrated during this period, the reported time-averaged static pressure rises due to the discharge will be consistently biased to values less than actual. If the pressure in the discharge due to joule heating is modeled as a step input and the time constant of the pressure transducer system is 11 s, integration over the last 15 s of the discharge would underestimate the equilibrium pressure by approximately 35%. This in no way, however, affects the observed trends in the data.

The temporal response of the discharge was evaluated by placing a pitot probe in the boundary layer. The pitot probe location was 0.5 cm above the plate surface at the rear edge of the downstream electrode, on the model centerline. In this case, the cathode was upstream. Figure 5 illustrates the pitot probe response for a discharge of approximately 10 s. When the discharge is turned off, the pitot pressure recovers to its predischarge values. The changes in pitot pressure when the discharge is turned off and on occur within one or two data points at the sampling frequency of 100 Hz. This response is much faster than the thermal response of the cathode and thus indicates that the observed effect for this discharge-on time or shorter periods on this model is due primarily to joule heating.

Figure 6 shows the effect of discharge power on surface pressures. These pressures are an average of the last 10 s of data with the discharge on. Although the effects are rather complex, several trends

Fig. 7 100 mA, 140 W discharge, point A in Fig. 6. View is from location downstream and above plate. Flow is from top-to-bottom, cathode is at top of image.

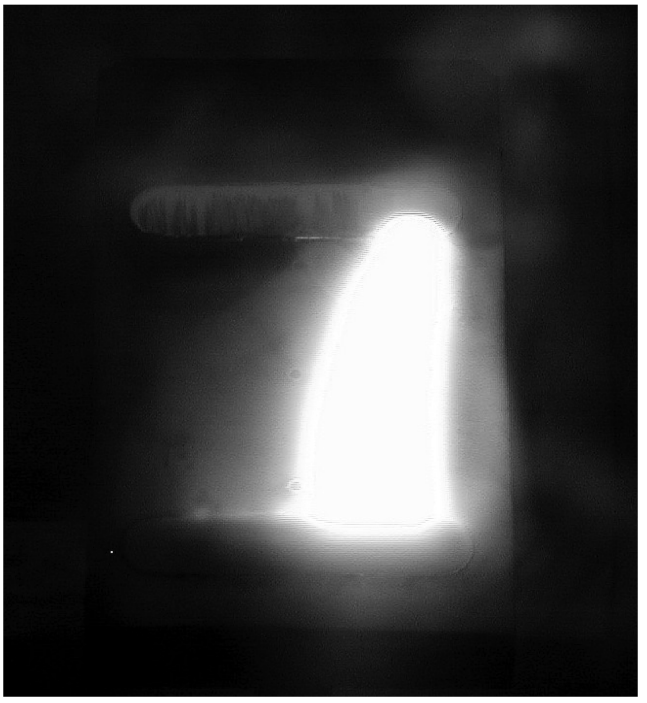

Fig. 8 400 mA, 170 W discharge, point B in Fig. 6.

are noted. In general, the surface pressure increase is roughly linear with power. This is especially evident for the two downstream pressure taps. The pressure tap nearest the cathode shows a more complex behavior. At this location, the pressure increases linearly with power, with the exception of outlier points near 60 and 140 W. The cluster of points near 60 W corresponds to 50 mA discharges. It was observed that at this current level the discharge was generally diffuse. This is also the case for the outlier point at 140 W (point A in Fig. 6). At other currents, the discharge had a tendency to constrict. This behavior is illustrated with images of the 140 W discharge in Fig. 7 and the 170 W discharge (point B in Fig. 6) in Fig. 8. The 140 W discharge is fairly diffuse and uniform, but the 170 W discharge shows a nonuniform, constricted structure on the right of the plate.

Presumably, the brighter portion of the 170 W discharge in Fig. 8 corresponds to a higher conductivity region with a higher current density. Locally higher heating is expected here, but because the discharge domain has shifted laterally, the pressure increment at tap 1 is less. At the more downstream stations, however, the pressure rise from the discharge has propagated laterally to the pressure taps on the model centerline. This explains the more regular trend of pressure versus power at these stations.

B. Effect of Magnetic Field on Applied Voltage

In this portion of the investigation, current, voltage, and surface pressures were recorded at a 2 Hz sampling rate. Data were acquired continuously during each 20-s discharge and for 20 s before and after. For cases with an applied magnetic field, the magnet was turned on and stabilized at a predetermined field strength before data were taken. Data were obtained at increasing magnetic field strengths until a discharge could no longer be maintained.

Voltage as a function of applied magnetic field for currents of 0.05, 0.1, 0.2, and 0.3 A are shown in Fig. 9. Negative currents refer to cases in which the upstream electrode is the cathode. The plotted voltages represent an average over the last 15 s of the discharge. For currents with magnitudes of 0.1–0.3 A, the voltage required to drive the current generally increases with increasing magnetic field. Within the scatter of the data, there is no dependence on the placement of the cathode. For 0.05 A current, the behavior is more complex. These data exhibit a great deal of scatter and show a trend of

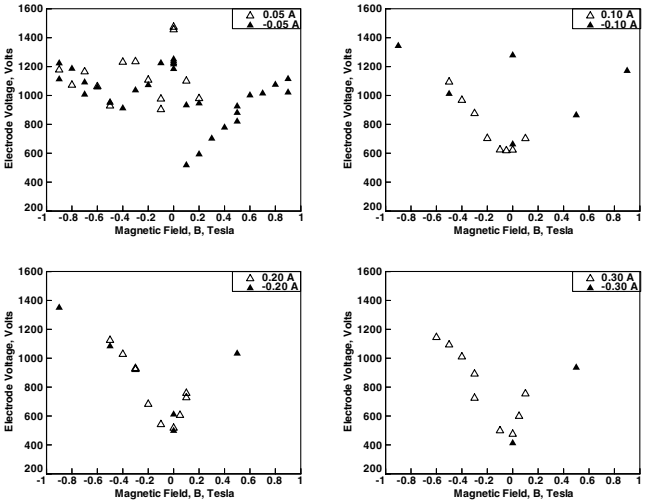

Fig. 9 Effect of magnetic field on voltage required to drive a given current.

decreasing voltage with increasing magnetic field for $-0.4 < B < 0.2T$. This is a region of high scatter in the data. Also, at $B = 0$, the voltage required to drive the current downstream is about 1400 V, compared with about 1200 V for current upstream. At higher magnetic fields, voltage increases with increasing magnetic field as it does at the other current levels.

The source of this behavior is a switch in the structure of the discharge from a generally diffuse to a more constricted discharge at higher currents and magnetic fields. Discharge images show that higher voltages are generally associated with the more diffuse discharges [24]. In some cases (for example, $B = 0.1T$ and 0.05 A) the images and voltage records indicate an unsteady switching between the two modes, so that the net result is an average of the two modes.

An estimate of the bulk fluid conductivity at zero magnetic field may be obtained by estimating the electric field and the current density. The electric field is assumed proportional to the applied voltage over the electrode separation, $V/\Delta x$, and the current density is assumed proportional to the total current divided by the electrode

area, J/A. A 0.05 A current at 1100 V implies a bulk conductivity of about 7×10^{-3} S/m. This is contrasted with a 500 V applied voltage for a 0.2 A current, implying an effective conductivity of 0.06 S/m. It must be stressed that these values are effective or bulk conductivities, for comparison purposes only. Most notably, the voltage drop through the electrode sheaths is not taken into account. Also, the electric field is nonuniform, especially near the cathode. Conductivity is also nonuniform. Langmuir probe measurements [24] show that the electron number density at a given height above the plate can vary an order of magnitude between the cathode and anode. A similar variation is observed in the vertical direction between the cathode and the edge of the discharge.

The increased voltage required to drive a given current in a magnetic field is consistent with a Hall effect. Given the relatively low density of the flow, a pronounced Hall effect is not unexpected. The current transverse to the magnetic field lines is $j_x = \sigma(E_x - \beta E_y)/(1 + \beta^2)$ [27]. Assuming that the fluid conductivity is independent of the applied electric field, data at $0.9T$ for a 0.2 A current compared to the zero magnetic field case indicate an effective Hall parameter of approximately 1.3. This value may be compared to an expected Hall parameter based on collision frequency data from Raizer [28]. Raizer cites a collision frequency of 3.9×10^9 per s per standard torr. With the freestream temperature a factor of 6 lower than ambient, this implies a collision frequency of 2.3×10^{10} per s at freestream densities. With [27] $\beta = eB/(m_e \nu)$, this implies a Hall parameter at $B = 0.9T$ of about 7, significantly higher than the value inferred from experimental measurements. Again, it must be stressed that the experimental value is a bulk parameter, and that the structure of the discharge varies significantly with the magnetic field. Also, it is questionable whether the conductivity remains constant with changes in applied electric field. Nevertheless, it is clear that the electron mobility is restricted across the magnetic field lines.

C. Effect of Magnetic Field on Surface Pressures

Surface pressures were recorded for a variety of magnetic field strengths and currents, and for all combinations of electrode and magnet polarities. For these cases the current vector is in the plane of the flat plate and directed either upstream or downstream. The magnetic field vector is also in the plane of the plate and transverse to the freestream velocity. The Lorentz force vector in this case is oriented either into or out of the plate surface, depending on the relative electric and magnetic field polarities. If the pressure induced by the discharge is due to a modification of the boundary-layer displacement thickness, then a Lorentz force oriented into the plate should suppress the pressure rise associated with joule heating, and a Lorentz force directed away from the plate should enhance the pressure rise, given sufficient interaction parameter.

Two factors combine to complicate interpretation of the magnet-on pressure measurements. First, to obtain high interaction parameters, high load factors, E/UB, were tested. The maximum load factor attained was over 500. At such high load factors, joule heating dominates the interaction. The dominance of joule heating and convection in and out of the plate surface make it difficult to separate heating from MHD effects. Second, as noted in the preceding section, the structure of the discharge changes with the application of a magnetic field, generally from a diffuse discharge at $B = 0$, to a more constricted discharge at higher values of B. Also, as noted next, the tendency of the discharge to follow magnetic field lines and Lorentz force vectoring of the plasma causes some of the visible discharge to appear around the sides of the model, rather than entirely on the top of the plate. The structure of the discharge strongly affects pressures at the most upstream tap [24]. At downstream locations, the pressure is less sensitive to the structure of the discharge, because the pressure signal from the discharge is able to propagate laterally to these taps.

Images of the discharges for $B = 0$ and $B = 0.9T$ in the positive and negative directions for 50 mA discharges are shown in Fig. 10. It is apparent that the magnetic field does indeed influence the shape of the discharge in the expected manner. A Lorentz force vector oriented into the plate suppresses the thickness of the glow above the plate. In fact, the discharge tends to spill over the plate surface and around the sides of the plate. Conversely, a Lorentz force vector oriented upwards tends to move the glow off the plate surface. For this case (Fig. 10, bottom), a dark region can be observed between the bright portion of the glow and the plate surface.

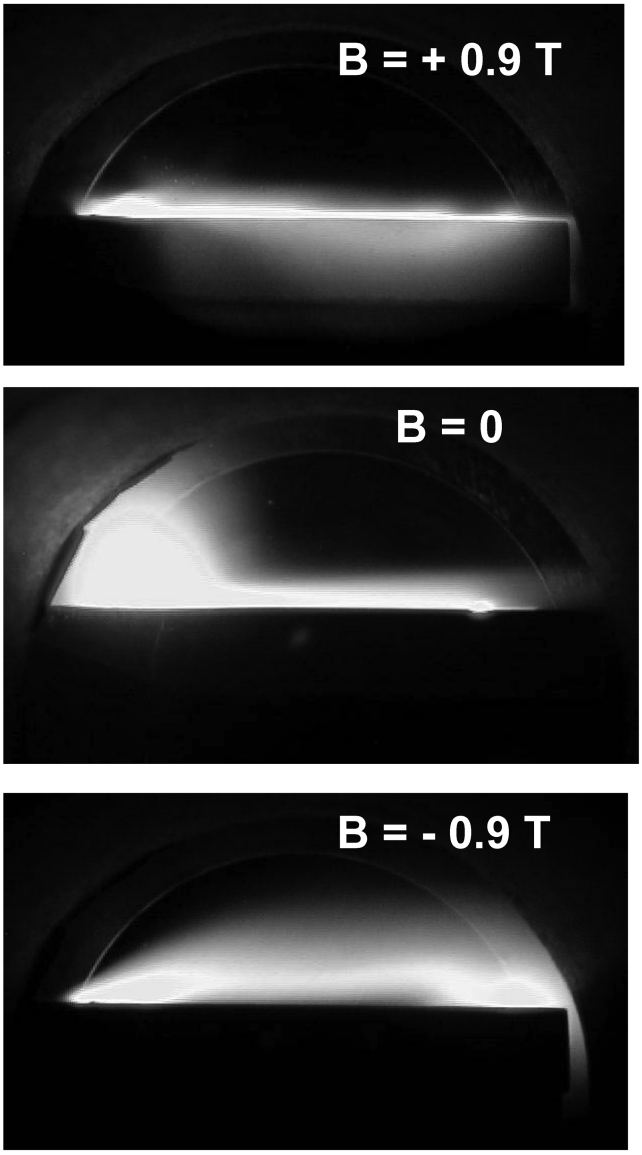

Fig. 10 Images showing the effect of transverse magnetic fields on the glow from a surface discharge. Flow is from left-to-right, cathode upstream.

The interaction parameter in the presence of an applied electric field is given as $I = (\sigma B^2 L/\rho U)(E/UB)$ [29,30]. The fluid conductivity and electric field are unknown and spatially nonuniform. An estimate of the bulk conductivity may be obtained from the overall current and electrode area, as discussed. The gas density and velocity are assessed at edge conditions. For this experiment, using the preceding assumptions, the interaction parameter is approximately $JB/26$. The maximum interaction parameter attained in this experiment, based on the preceding assumptions, was 0.009.

It should be noted that the use of edge values gives a low estimate of the interaction parameter. Analysis of experiments by Henoch and Stace [6] on MHD control of turbulent electrolyte, flat-plate boundary layers showed that the friction velocity was an appropriate velocity scale for a modified interaction parameter. Macheret et al. [31] have also suggested using u^* as a velocity scale in the interaction parameter for boundary-layer flows. Meyer et al. [32] applied it to experimental compressible flow data. All other conditions being equal, the interaction parameter for an applied electric field based on

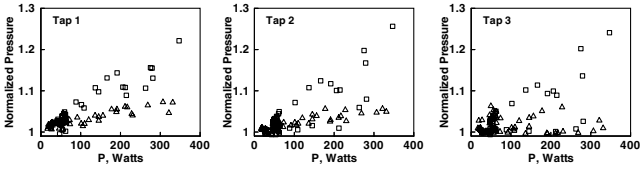

Fig. 11 Induced pressure at each measuring station as a function of power. Squares, cathode upstream; triangles, cathode downstream. Magnetic field varies from −0.9 to 0.9 T.

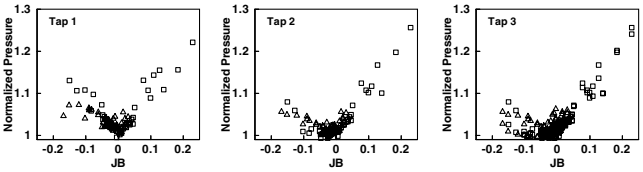

Fig. 12 Pressure induced by the discharge at each measuring station plotted vs the product of current and magnetic field.

u^* rather than U is larger by a factor of $(U/u^*)^2$. For the current experiments, this ratio is 280, and the largest value of I^* obtained is 2.5, based on a friction velocity derived from a similarity solution for a laminar boundary layer.

For laminar flows, I^* is also simply related to the Hartmann number [33], which is conventionally used to describe laminar MHD shear layers. For laminar, flat-plate boundary layers, the skin friction is proportional to the inverse square root of the length Reynolds number, $c_f = C_1 Re^{-1/2}$. The length scale for the Hartmann number is some measure of the shear layer thickness, but for a laminar flat-plate boundary layer the ratio of velocity thickness to streamwise dimension is inversely proportional to the square root of the Reynolds number, $(\delta/L) = C_2 Re^{-1/2}$. With these substitutions, the interaction parameter based on friction velocity is $I^* = (Ha/C_2)^2 \sqrt{2/C_1} Re^{1/4}$. For the conditions of these experiments, a laminar boundary-layer similarity solution gives $C_1 = 0.65$ and $C_2 = 15.8$.

The ratio of the Lorentz force to viscous forces on a fluid element is equal to the square of the Hartmann number times the load factor. For the conditions of this experiment, $Ha^2 E/UB \approx 40JB$. The maximum Hartmann number obtained in this experiment is approximately nine, indicating that the maximum Lorentz force achieved is significant compared to viscous forces in the boundary layer.

Given the strong effect of joule heating and the tendency for surface pressures to scale on applied power [24] in the absence of a magnetic field, the induced pressure was plotted as a function of applied power (Fig. 11) for various magnetic fields. If changes in the induced pressure are due to changes in joule heating, plotting pressure versus power would be expected to collapse the data. Overall, induced pressure increases with increasing power input, but the scatter in the data is quite high. Except for tap 3 at powers below 90 W, the cathode-downstream discharges create a lesser pressure rise. This change in behavior of the tap 3 pressure is probably correlated with a change from a diffuse to a constricted discharge.

Figure 12 shows the induced pressure for each tap as a function of total current times magnetic field, which, as shown, may be related to some measure of bulk interaction parameter. The sign of JB is retained to differentiate between the Lorentz force into the plate ($JB < 0$) and Lorentz force out of the plate ($JB > 0$) cases. Cases with $B = 0$ are not plotted, because they were obtained at various powers and do not scale in this coordinate system. Scatter is present, but is considerably reduced compared to scaling with power. The Lorentz force direction has little effect on the most upstream tap pressure. Tap 2 pressures show some effect of the Lorentz force vector direction. A Lorentz force into the plate reduces the pressure rise, compared with a Lorentz force out of the plate. This trend is further emphasized for tap 3. In some cases the pressure rise at tap 3 is completely negated by the magnetic field.

This result is consistent with the expected behavior of a Lorentz force. However, given the significant changes in discharge structure with magnetic field, and the strong effect of joule heating, it cannot be ruled out that the observed magnetic field effects are due in part or whole to changes in joule heating from the magnetic field. Figure 10 shows that at least part of the discharge moves around the sides of the plate for a sufficiently high field. Nevertheless, the effects observed in Fig. 12 show a pronounced and repeatable coupling between the applied magnetic field and the surface pressure.

IV. Conclusion

Surface discharges are shown to be an effective means of manipulating the pressure field about a flat plate. The configuration demonstrated in this paper could have applications as a virtual flap or boundary-layer diverter. The observed effect is due to joule heating of the boundary-layer fluid near the cathode. The heated fluid expands and deflects the external flow. Although there is some convective heat transfer from the electrode to the gas, for discharges of less than several seconds the bulk of the observed effect is due to joule heating of the fluid.

In the absence of a magnetic field, the pressure increment due to the discharge scales roughly linearly with the discharge power for the range of parameters considered. In general, the pressure increment near the cathode was higher for more diffuse discharges. A constriction in the discharge had a pronounced effect on the pressure near the cathode, but had a lesser effect downstream. This is presumed to be due to the nonuniformity of the discharge near the cathode.

For the configuration tested, the discharge tends toward a diffuse discharge for currents of less than 100 mA and magnetic fields less than about 0.2 T. Higher currents and magnetic fields create a more constricted discharge. When the discharge is constricted, increased voltage is required to drive a fixed current in the presence of an applied magnetic field. Although this observation is consistent with a Hall effect, the measured effective Hall parameter is less than that predicted using published values for collision frequency. This discrepancy is probably due to changes in the structure and conductivity of the discharge which are not accounted for in calculation of an effective Hall parameter.

Observation of the glow from the discharge indicated that a Lorentz force oriented into the plate pushed the discharge downwards, and a Lorentz force vector oriented upwards pushed the discharge away from the plate. Surface pressures on the plate were affected accordingly. The pressure rise was enhanced in the presence of an upwards-oriented Lorentz force, and negated when the Lorentz force vector was oriented downwards. This effect is more pronounced with increasing distance along the plate. This effect is consistent with a Lorentz force changing the boundary-layer thickness. However, given the three-dimensional nature of the discharge, the alteration of the discharge with magnetic field, and the strong joule heating of the boundary layer, it cannot be ruled out that this effect is due to a change in joule heating with the applied magnetic field. Nevertheless, the observations show a consistent effect of the magnetic field on the pressure field created by the discharge.

Acknowledgments

The authors wish to acknowledge the support of the Integration Branch of the Air Force Research Laboratory's Air Vehicles Directorate for support of plasma channel operations. The authors also wish to thank the personnel of General Dynamics and Veridian for tunnel operations, and James Crafton and Sergey Fonov of ISSI for his temperature-sensitive paint measurements. This work was supported by John Schmisseur of the Air Force Office of Scientific Research.

References

[1] Kantrowitz, A. R., "A Survey of Physical Phenomena Occurring in Flight at Extreme Speeds," *Proceedings of the Conference on High-Speed Aeronautics*, edited by A. Ferri, N. J. Hoff, and P. A. Libby, Polytechnic Institute of Brooklyn, New York, 1955, 335–339.

[2] Resler, E. L., Jr., and Sears, W. R., "The Prospects for Magneto-Aerodynamics," *Journal of the Aeronautical Sciences*, Vol. 25, No. 4, April 1958, pp. 235–245, 258.
[3] Gurjanov, E. P., and Harsha, P. T., "AJAX: New Directions in Hypersonic Technology," AIAA Paper 96-4609, Nov. 1996.
[4] Kimmel, R. L., "Aspects of Hypersonic Boundary Layer Transition Control," AIAA Paper 2003-0772, Jan. 2003.
[5] Palm, P., Meyer, R., Plönjes, E., Bezant, A., Adamovich, I. V., Rich, J. W., and Gogineni, S., "MHD Effect on a Supersonic Weakly Ionized Flow," AIAA Paper 2002-2246, May 2002.
[6] Henoch, C., and Stace, J., "Experimental Investigation of a Salt Water Turbulent Boundary Layer Modified by an Applied Streamwise Magnetohydrodynamic Body Force," *Physics of Fluids*, Vol. 7, No. 6, June 1995, pp. 1371–1383.
[7] Roth, J. R., Sherman, D. M., and Wilkinson, S. P., "Electrohydrodynamic Flow Control with a Glow-Discharge Surface Plasma," *AIAA Journal*, Vol. 38, No. 7, July 2000, pp. 1166–1172.
[8] Artana, G., D'Adamo, J., Léger, L., Moreau, E., and Touchard, G., "Flow Control with Electrohydrodynamic Actuators," AIAA Paper 2001-0351, 2001.
[9] Léger, L., Moreau, E., and Touchard, G., "Electrohydrodynamic Airflow Control Along a Flat Plate by a DC Surface Corona Discharge —Velocity Profile and Wall Pressure Measurements," AIAA Paper 2002-2833, 2002.
[10] Corke, T. C., Jumper, E. J., Post, M. L., Orlov, D., and McLaughlin, T. E., "Application of Weakly-Ionized Plasmas as Wing Flow-Control Devices," AIAA Paper 2002-0350, Jan. 2002.
[11] Post, M. L., and Corke, T. C., "Separation Control on High Angle of Attack Airfoil Using Plasma Actuators," AIAA Paper 2003-1024, Jan. 2003.
[12] Hultgren, L. S., and Ashpis, D. E., "Demonstration of Separation Delay with Glow-Discharge Plasma Actuators," AIAA Paper 2003-1025, Jan. 2003.
[13] Roth, J. R., Sin, H., Madhan, R. C. M., and Wilkinson, S. P., "Flow Re-Attachment and Acceleration by Paraelectric and Peristaltic Electrohydrodynamic (EHD) Effects," AIAA Paper 2003-531, Jan. 2003.
[14] Johnson, G. A., and Scott, S. J., "Plasma-Aerodynamic Boundary Layer Interaction Studies," AIAA Paper 2001-3052, 2001.
[15] Wilkinson, S. P., "Investigation of an Oscillating Surface Plasma for Turbulent Drag Reduction," AIAA Paper 2003-1023, Jan. 2003.
[16] Macheret, S. O., Shneider, M. N., and Miles, R. B., "Magneto-hydrodynamic and Electrohydrodynamic Control of Hypersonic Flows of Weakly Ionized Plasmas," AIAA Paper 2002-2249, May 2002.
[17] Shibkov, V. M., Alexandrov, A. F., Chernikov, A. V., Ershov, A. P., Georgievskiy, P. Yu., Gromov, V. G., Larin, O. B., Levin, V. A., Shibkova, L. V., Timofeev, I. B., Voskanyan, A. V., and Zlobin, V. V., "Influence of the Surface Microwave Discharge on the Parameters of Supersonic Airflow Near a Dielectric Body," AIAA Paper 2003-1192, Jan. 2003.
[18] Leonov, S., Bityurin, V., Savischenko, N., Yuriev, A., and Gromov, V., "Influence of Surface Electric Discharge on Friction of Plate in Subsonic and Transonic Airflow," AIAA Paper 2001-0640, Jan. 2001.
[19] Leonov, S., Bityurin, V., Klimov, A., Kolesnichenko, Y., and Yuriev, A., "Influence of Structural Electric Discharges on Parameters of Streamlined Bodies in Airflow," AIAA Paper 2001-3057, June 2001.
[20] Leonov, S., Bityurin, V., Savelkin, K., and Yarantsev, D., "Effect of Electrical Discharge on Separation Processes and Shocks Position in Supersonic Airflow," AIAA Paper 2002-0355, Jan. 2002.
[21] Leonov, S., Bityurin, V., Savelkin, K., and Yarantsev, D., "Progress in Investigation for Plasma Control of Duct-Driven Flows," AIAA Paper 2003-0699, Jan. 2003.
[22] Leonov, S., Bityurin, V., and Yarantsev, D., "The Effect of Plasma Induced Separation," AIAA Paper 2003-3853, June 2003.
[23] Menart, J. A., Shang, J., Kimmel, R. L., and Hayes, J. R., "Effects of Magnetic Fields on Plasmas Generated in a Mach 5 Wind Tunnel," AIAA Paper 2003-4165, June 2003.
[24] Kimmel, R. L., Hayes, J. R., Menart, J., and Shang, J. S., "Effect of Surface Plasma Discharges on Boundary Layers at Mach 5," AIAA Paper 2004-0509, Jan. 2004.
[25] Kimmel, R. L., Hayes, J. R., Menart, J. A., and Shang, J. "Effect of Magnetic Fields on Surface Plasma Discharges at Mach 5," AIAA 2004-2661, June 2004.
[26] Shang, J. S., Kimmel, R., Hayes, J., and Tyler, C., "Performance of a Low-Density Hypersonic Magneto-Aerodynamic Facility," AIAA Paper 03-0329, Jan. 2003.
[27] Rosa, R. J., *Magnetohydrodynamic Energy Conversion*, McGraw–Hill Book Company, New York, 1968, pp. 24–31.
[28] Raizer, Yuri P., *Gas Discharge Physics*, Springer–Verlag, New York, 1997, p. 11.
[29] Crawford, C. H., and Karniadakis, G. E., "Control of External Flows via Electro-Magnetic Fields," AIAA Paper 95-2185, June 1995.
[30] Weier, T., Gerbeth, G., Mutschke, G., Platacis, E., and Lielausis, O., "Experiments on Cylinder Wake Stabilization in an Electrolyte Solution by Means of Electromagnetic Forces Localized on the Cylinder Surface," *Experimental Thermal and Fluid Science*, Vol. 16, Nos. 1–2, Jan.–Feb. 1998, pp. 84–91.
[31] Macheret, S. O., Shneider, M. N., and Miles, R. B., "Magneto-hydrodynamic and Electrohydrodynamic Control of Hypersonic Flows of Weakly Ionized Plasmas," AIAA Paper 2002-2249, May 2002.
[32] Meyer, R., McEldowney, B.,, Chintala, N., and Adamovich, I. V., "Measurements of Electrical Parameters of a Supersonic Non-equilibrium MHD Channel," AIAA Paper 2003-4279, June 2003.
[33] Ostrach, S., "Laminar Flows with Body Forces," *High Speed Aerodynamics and Jet Propulsion, Vol. 4, Theory of Laminar Flows*, edited by F. K. Moore, Princeton Univ. Press, Princeton, NJ, 1964.

A. Ketsdever
Associate Editor